

## Effects of thioureido imidazoline on the passivation and pitting corrosion of N80 steel in CO<sub>2</sub>-saturated NaCl-NaNO<sub>2</sub> solution

Jingmao Zhao<sup>1,2,\*</sup>, Feng Gu<sup>1</sup>, Denghui Wang<sup>1</sup>, Miao Yu<sup>1</sup>

<sup>1</sup> College of Material Science and Engineering, Beijing University of Chemical Technology, Beijing 100029, China

<sup>2</sup> Beijing Key Laboratory of Electrochemical Process and Technology for Materials, Beijing 100029, China

\*E-mail: [jingmaozhao@126.com](mailto:jingmaozhao@126.com)

Received: 14 October 2017 / Accepted: 16 December 2017 / Published: 5 February 2018

---

The effects of thioureido imidazoline (TAI) corrosion inhibitor on the passivation and pitting corrosion of N80 steel in CO<sub>2</sub>-saturated NaCl-NaNO<sub>2</sub> solution were studied by potentiodynamic polarization, electrochemical noise (EN), and wire beam electrode (WBE) measurements. The results suggest that TAI showed two opposite effects, e.g., promoting the passivation of steel electrode while decreasing the pitting potential of N80 steel, possibly due to the adsorption and desorption of the inhibitor on/from the steel surface. TAI was able to slow down the general corrosion rate in the solution as an anodic inhibitor.

---

**Keywords:** Thioureido imidazoline; N80 steel; CO<sub>2</sub> corrosion; Passivation; Pitting corrosion

### 1. INTRODUCTION

Injecting corrosion inhibitors is one of the most economical and effective methods to minimize the corrosion of steel equipment and pipelines for crude oil production and transportation. However, it has been reported that an inappropriate application of corrosion inhibitors can cause pitting corrosion instead. For example, Han *et al.* investigated the corrosion of L245 carbon steel in H<sub>2</sub>S-containing brine and found no pitting corrosion of the steel immersed in a brine solution, but serious pitting corrosion occurred at a corrosion rate of 52 mm/a when imidazoline quaternary ammonium salt (90 mg/L) was added to the brine solution[1]. The pitting corrosion was inhibited when imidazoline quaternary ammonium salt was used together with a surfactant, even for 168 h. They explained that imidazoline quaternary ammonium salt at a low concentration could not form an integrated and dense corrosion inhibitor film. The bare area acted as an anode and the inhibitor covering the area acted as a cathode, forming a galvanic cell that caused the pitting corrosion. The surfactant could improve the

dispersion of the corrosion inhibitor to form a homogenous integrated inhibitor film on the steel surface, which inhibited the pitting corrosion. Tan *et al.* studied the corrosion inhibition behaviors of imidazoline and resorcinarene acid in CO<sub>2</sub>-saturated 3% NaCl solution using a 10×10 electrode array and found that imidazoline reduced the number of anodes, and the corrosion mainly occurred on the anodes[2]. The susceptibility to localized corrosion increased as the maximum current density on the anode increased. The addition of resorcinarene acid produced more randomly distributed anodes, which reduced the susceptibility to localized corrosion. Lucio-Garcia *et al.* investigated the corrosion inhibition effects of different concentrations of hydroxyethyl imidazoline in H<sub>2</sub>S-containing 3% NaCl solution and found that less than 10 mg/L of the inhibitor caused the highest susceptibility to localized corrosion due to the formation of a porous inhibitor film on the steel surface[3]. Both localized corrosion and general corrosion co-occurred at corrosion inhibitor concentrations of 50 mg/L and 100 mg/L.

Imidazoline derivatives have been successfully used as corrosion inhibitors to prevent CO<sub>2</sub> and H<sub>2</sub>S corrosion in oil-gas fields. 1-(2-thioureidoethyl)-2-alkyl imidazoline (TAI) has been well studied as a corrosion inhibitor for carbon steel in CO<sub>2</sub>-containing brine solutions. TAI contains multiple nitrogen atoms and one sulfur atom, which can form multi-center chemical absorption sites on the steel surface and thus provide satisfactory corrosion inhibition abilities. The inhibition mechanism of TAI on the corrosion of carbon steel has been studied in CO<sub>2</sub> saturated brine solutions[4-5]. The results indicated that the inhibitor was a mixed-type inhibitor that preferentially retarded the anodic process. The inhibition efficiency increased first, peaked at 0.15 mmol/L, and then decreased with the increase of inhibitor concentration due to the change of adsorption mode. TAI can be used as an effective inhibitor against CO<sub>2</sub> corrosion in both gas and liquid phases[6]. The adsorption of TAI molecules on Q235 steel surface can be fitted by the Frumkin isotherm equation[7]. The quantum chemistry calculation results revealed that the imidazoline ring and heteroatoms were the active sites[8]. A recent study on the inhibition behaviors of TAI against flow accelerated corrosion at different locations of an X65 carbon steel elbow in a CO<sub>2</sub>-saturated solution suggests that TAI is an anodic inhibitor and the inhibition efficiency at the inner wall of the steel elbow is lower than that at the outer wall[9].

Most of the previous works focused on the effects of inorganic inhibitors (such as chromate, molybdate and phosphate) on the passivation/pitting behavior of iron[10-11], but few works have investigated organic inhibitors. For example, the stability of a passive film of iron electrode formed by chromate is the best, followed by nitrite and then bicarbonate. MoO<sub>4</sub><sup>2-</sup> ions can suppress both pit nucleation and propagation of mild steel in a bicarbonate solution containing Cl<sup>-</sup>, while Cr<sub>2</sub>O<sub>7</sub><sup>2-</sup> ions can suppress pit nucleation but stimulate pit growth. We previously investigated the effects of TAI on the passivation and pitting corrosion of X60 steel in a NaCl-NaNO<sub>2</sub> solution without removing oxygen [12]. The results suggested that TAI can promote the passivation of X60 steel in the solution but decrease the pitting potential due to the preferential adsorption of thiourea molecules. Because most oil-gas productions are conducted in oxygen-free environments, in the present work, the effects of TAI on the passivation and pitting corrosion of N80 steel in a CO<sub>2</sub>-saturated NaCl-NaNO<sub>2</sub> solution were further studied by potentiodynamic polarization, electrochemical noise (EN) and wire beam electrode (WBE) measurements.

## 2. EXPERIMENTAL METHODS

### 2.1 Sample preparation

N80 steel was used as the studied material with the following composition (wt%): C 0.24, Mn 1.19, Si 0.22, P 0.013, S 0.004, Cr 0.036, Mo 0.021, Ni 0.028, V 0.017, Cu 0.019 and Fe bal. A N80 steel rod with a diameter of 1 cm was cut into 0.5-cm-thick pieces. The sample was sealed with epoxy resin with an area of 0.785 cm<sup>2</sup> exposed as the working area. The working area was polished with 240-1000# silicon carbon abrasive papers step by step, washed with deionized water, and degreased with acetone.

Because the steel is active in 0.2 mol/L NaCl solution, NaNO<sub>2</sub> was added at a concentration of 0.2 mol/L into the solution in order to passivate the steel. The test solution was prepared with analytical grade NaCl and NaNO<sub>2</sub> along with deionized water.

The corrosion inhibitor, TAI, was synthesized as described elsewhere[13]. Its molecular structure, as shown in Fig. 1, where R represents alkyl C<sub>17</sub>H<sub>35</sub>, was confirmed by FT-IR analysis. The concentration of TAI in the test solution varied from 0 to 200 mg/L.

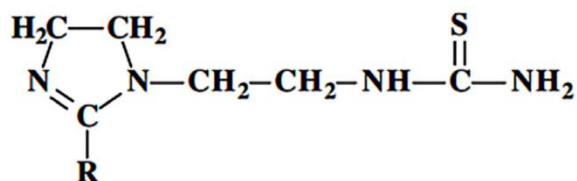


**Figure 1.** Molecular structure of thioureido imidazoline

### 2.2 Potentiodynamic polarization measurement

The potentiodynamic polarization curves of the steel in the test solutions containing different concentrations of TAI were measured using a potentiostat in a 500-ml round-bottom flask equipped with a Pt electrode as the counter electrode, a saturated calomel electrode (SCE) as the reference electrode, and N80 steel as the working electrode (WE). Before each test, the test solution was bubbled with CO<sub>2</sub> gas for 2 h to remove oxygen. The pH of the bubbled solution was measured to be 4.94. The WE was then placed into the solution, and the solution was constantly bubbled with CO<sub>2</sub> to maintain a virtually oxygen-free environment. The WE was immersed in the solution for 30 min, allowing the WE to reach a stable state with the fluctuation of open circuit potential (OCP) less than ±5 mV before the measurement was started. The potential was scanned from -100 mV vs. OCP in the anodic direction at a scan rate of 0.5 mV/s. Slower scanning rates showed no significant effect on the polarization curve shape. Each measurement was conducted in triplicate.

As the polarization entered in the anodic dissolution region, further increasing the anodic polarization caused a rapid decline in the anodic current, and the steel became passive. The highest current density at the active dissolution region is denoted as  $i_{\text{peak}}$ . For more noble potentials, an abruptly increased current indicated that broken or pitting potential ( $E_b$ ) was reached. The scanning

potential was reversed as the current density reached  $4 \text{ mA/cm}^2$  and was continued until the current density returned to the repassivation current at the repassivation potential ( $E_p$ ).

### 2.3 Electrochemical noise measurement

Electrochemical noise (EN) was measured using a three-electrode system consisting of two identical N80 electrodes, WE1 and WE2, and a SCE as the reference electrode. Before each test, the test solution was deaerated as described above. After the steel was immersed in the test solution for 24 h, the potential and current curves were recorded simultaneously at a sampling rate of 4 points per second for a period of 2048 s using a zero-resistance ammeter connected to a personal computer. To avoid external signal interferences, all EN measurements were conducted in a Faraday shielding box. The DC trend was removed from the raw data by the least-square fitting method reported by Tan *et al.*[14]

### 2.4 Wire beam electrode (WBE)

The WBE was made with 100 identical N80 steel wires with a diameter of 0.5 mm in a  $10 \times 10$  array. The wires were insulated 2 mm from each other using epoxy resin (Figure 2). Before each measurement, the working electrode was mechanically polished with 240-2000 # emery paper, rinsed with deionized water and ethanol, and immersed in 800 mL of test solution. The test solution was deaerated as described above. The corrosion was monitored by mapping the galvanic currents between a chosen wire and all the other wires sorted together using a pre-programmed autoswitch device and an ACM AutoZRA. The galvanic current was measured and analyzed as described in the literature[15]. The corrosion potential of each wire was also measured using a SCE as the reference electrode to determine the inhibition mechanism of TAI inhibitor. The test was continued for 10 h and measured at an interval of 1 h for the potentials and galvanic currents on the 100 electrodes. All the experiments were carried out at room temperature ( $\sim 25^\circ\text{C}$ ).

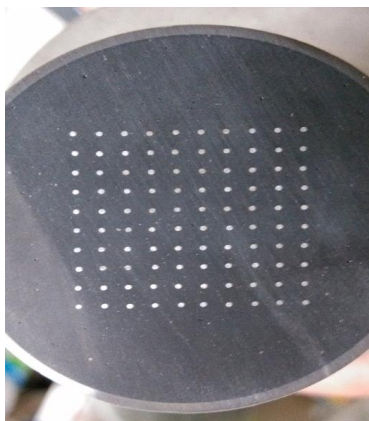


**Figure 2.** Photo of a wire beam electrode (WBE)

### 3. RESULTS AND DISCUSSION

#### 3.1 Potentiodynamic polarization

Fig. 3 shows the potentiodynamic polarization curves of N80 steel in the CO<sub>2</sub>-saturated NaCl (0.2 mol/L) + NaNO<sub>2</sub> (0.2 mol/L) solutions containing different concentrations of TAI. The anodic polarization curves exhibited typical passivation behaviors characterized by active dissolution, passive, and transpassive regions. The parameters, including corrosion potential ( $E_{\text{corr}}$ ), corrosion current density ( $i_{\text{corr}}$ ),  $E_b$ ,  $E_p$ , and  $i_{\text{peak}}$ , can be used to represent the passivation behavior of the steel. As seen from Fig. 3 and Table 1,  $E_{\text{corr}}$  gradually moved to the positive direction, suggesting that TAI was an anodic inhibitor. The  $i_{\text{corr}}$ , determined by fitting the weak polarization zones of curves using the Gauss-Newton method, represents the general corrosion rate. It decreased as TAI was added, indicating that TAI inhibited the general corrosion to a certain extent. The effects of TAI on passivation and pitting corrosion seemed to be contradictory. On one hand,  $i_{\text{peak}}$  decreased with the increase of TAI concentration, indicating that TAI promoted the passivation of the steel. On the other hand, the addition of TAI decreased  $E_b$ , and increased the passive current densities slightly, indicating that it promoted pitting corrosion, which is consistent with our previous results[12]. This can be explained by the fact that at low applied anodic potentials, i.e., in the active dissolution and transition regions, TAI molecules were adsorbed on the steel surface, thus reducing  $i_{\text{peak}}$ . The adsorbed inhibitor molecules were desorbed from the passive film as the applied potential increased, leaving defects in the film. The Cl<sup>-</sup> ions were preferentially adsorbed on the defects and attacked the passive film, resulting in a lower  $E_b$  than that in the blank solution (without TAI).

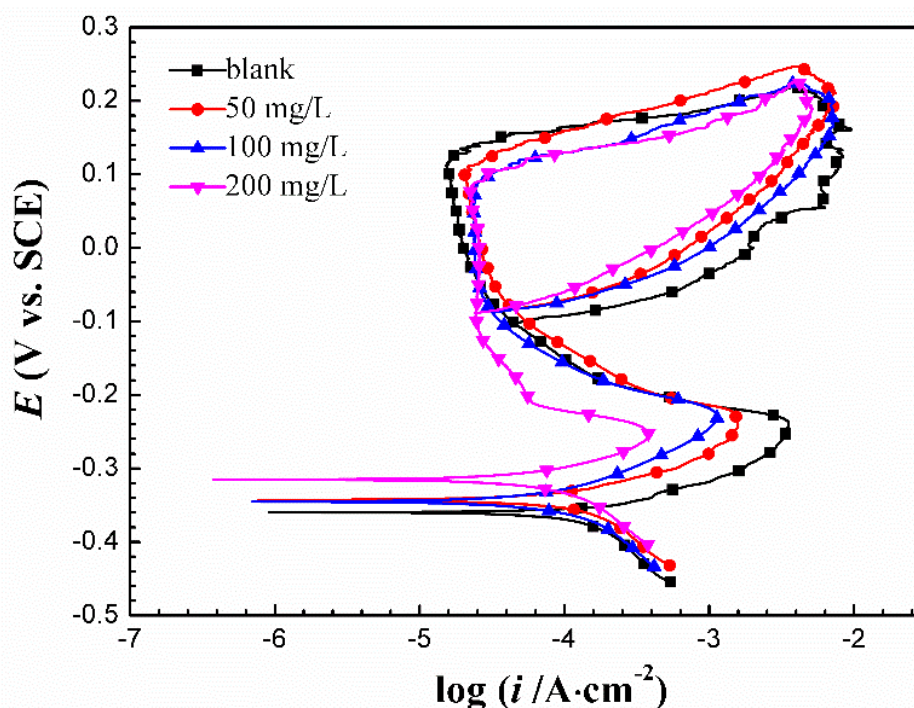


**Figure 3.** Potentiodynamic polarization curves of N80 steel in the CO<sub>2</sub>-saturated NaCl (0.2 mol/L) + NaNO<sub>2</sub> (0.2 mol/L) solutions containing different concentrations of TAI

**Table 1.** Electrochemical polarization parameters of N80 steel in the CO<sub>2</sub>-saturated NaCl (0.2 mol/L) + NaNO<sub>2</sub> (0.2 mol/L) solutions containing different concentrations of TAI

Concentration of TAI (mg/L)	$E_{\text{corr}}$ (mV <sub>SCE</sub> )	$i_{\text{corr}}$ (mA/cm <sup>2</sup> )	$E_{\text{b}}$ (mV <sub>SCE</sub> )	$E_{\text{p}}$ (mV <sub>SCE</sub> )	$i_{\text{peak}}$ (mA/cm <sup>2</sup> )
0	-357.0	0.2068	114.6	-97.5	3.80
50	-338.1	0.1672	96.6	-83.2	1.66
100	-344.8	0.1280	86.6	-89.8	1.17
200	-313.9	0.0992	84.5	-90.1	0.40

### 3.2 Electrochemical noise

The electrochemical noise technique has been used to study the metastable pitting process taking place on metals. The electrochemical parameters, such as noise resistance ( $R_n$ )<sup>[3]</sup>, localization index (LI)<sup>[3]</sup>, and Hurst exponent (H.)<sup>[16]</sup>, can be determined by electrochemical noise measurement. These parameters vary with some variables, including the concentration of corrosive or inhibitive ions, the test temperature, pH value of solution and so on, which can provide important information of corrosion kinetics, especially those involving localized corrosions.

Electrochemical noise resistance ( $R_n$ ) can be calculated by Equation 1<sup>[3]</sup>:

$$R_n = S_v/S_i \quad (1)$$

where  $S_v$  and  $S_i$  are the standard deviations of potential and current, respectively. The value of  $R_n$  can be considered as a linear polarization resistance ( $R_p$ )<sup>[3]</sup>. According to the Stern-Geary equation, it is inversely proportional to corrosion rate.

Figs. 4 and 5 show the potential and current fluctuation characteristics of the steel electrode after immersion in solutions with different concentrations of TAI for 24 h. Table 2 lists the obtained standard deviations of potential and current along with the electrochemical noise resistance of N80 steel. It is noted that the standard deviations of current or potential fluctuation decreased by a factor of 10<sup>1</sup> or 10<sup>2</sup> in the presence of TAI. However, the frequencies of the current or potential fluctuations for the steel in the solutions with TAI are very high, suggesting that more metastable pitting events occur on the steel surface.

It can be seen from Table 2 that  $R_n$  increases with the increase of TAI concentration, suggesting that the corrosion of N80 steel was inhibited by TAI. This is in good agreement with the polarization results.

The localization index (LI) can be calculated by Equation 2<sup>[3]</sup>:

$$LI = S_i / I_{rms} \tag{2}$$

where  $I_{rms}$  is the root mean square value of the current. LI is correlated with the tendency towards localized or general corrosion. An LI value between 1 and 0.1 suggests a high susceptibility to localized corrosion, and the higher the value, the higher the susceptibility to localized corrosion. An LI value between 0.01 and 0.001 indicates a high susceptibility to uniform corrosion. An LI value between 0.1 and 0.01 suggests the susceptibility of the alloy to mixed localized and general corrosion.

As shown in Table 2, LI increases with the increase of TAI concentration, indicating that the susceptibility to pitting corrosion increases with the increase of TAI concentration, consistent with the results of potentiodynamic polarization measurements

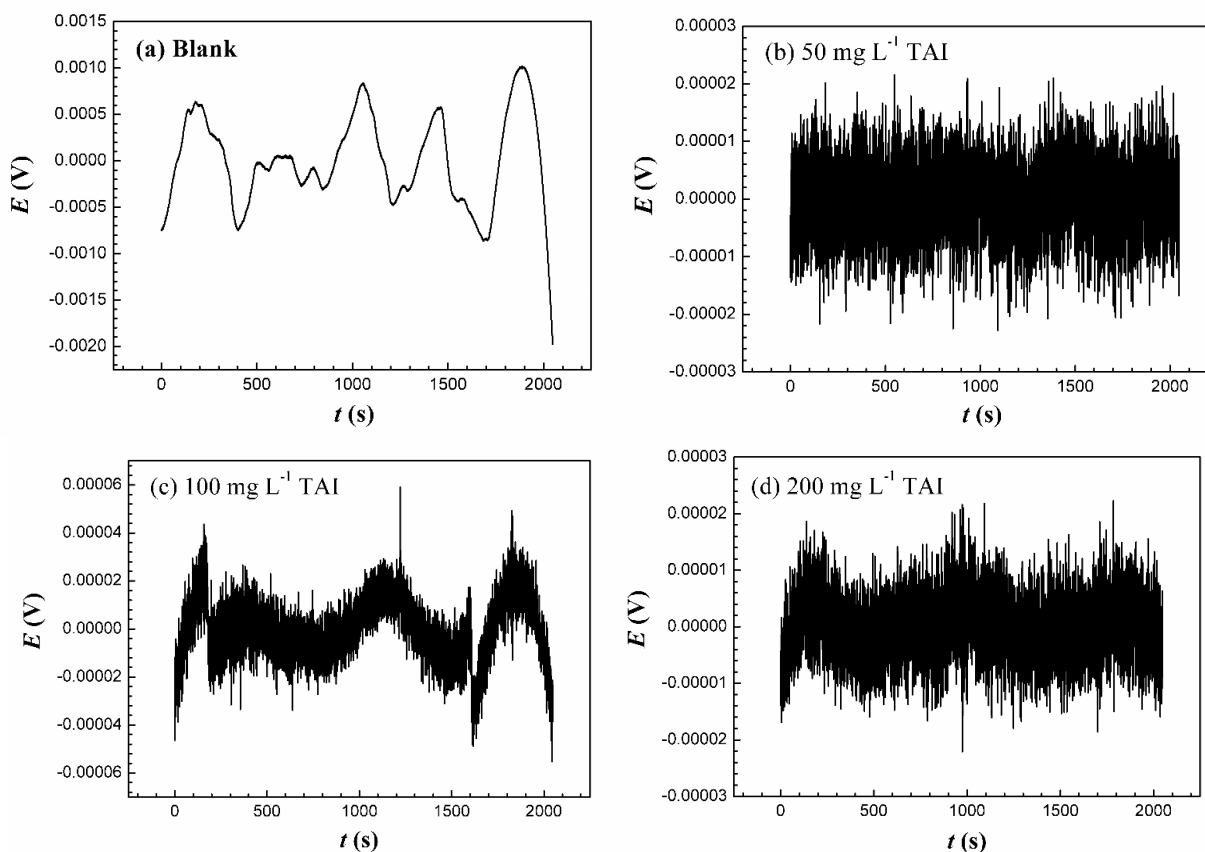


**Figure 4.** DC trend removed potentials vs time of N80 steel in the test solutions containing different concentrations of TAI

**Table 2.** Electrochemical noise parameters of N80 steel in the CO<sub>2</sub>-saturated NaCl (0.2 mol/L) + NaNO<sub>2</sub> (0.2 mol/L) solutions containing different concentrations of TAI

Concentration of TAI (mg/L)	$S_i$	$S_v$	$R_n$ (ohm.cm <sup>2</sup> )	LI
0	$3.03 \times 10^{-7}$	$2.28 \times 10^{-4}$	752	0.6803
50	$4.24 \times 10^{-9}$	$5.79 \times 10^{-6}$	1365	0.9078
100	$3.16 \times 10^{-9}$	$4.68 \times 10^{-6}$	1481	0.9797
200	$2.44 \times 10^{-9}$	$1.30 \times 10^{-5}$	5328	0.9989

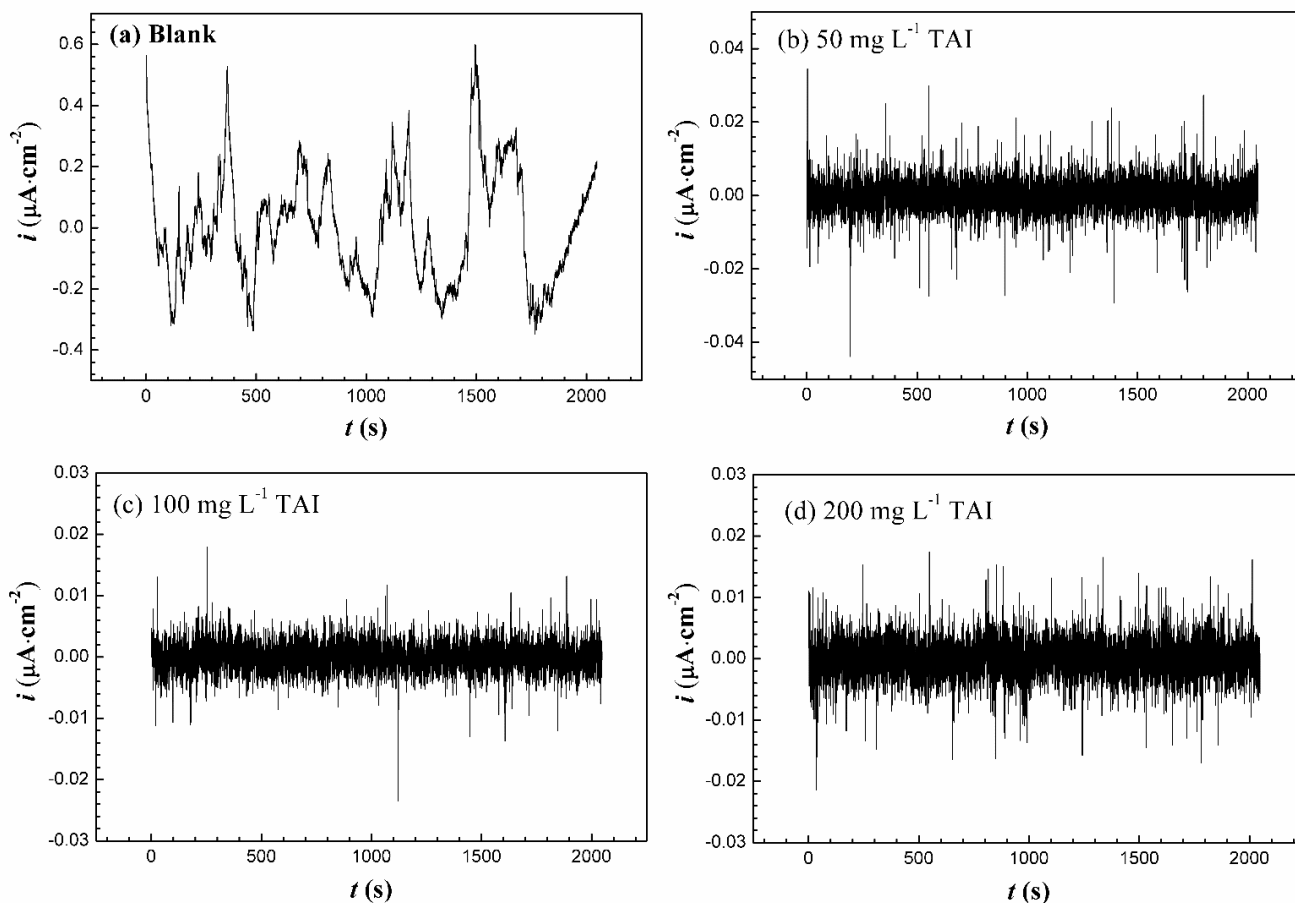


**Figure 5.** DC trend removed current vs time of N80 steel in the test solutions containing different concentrations of TAI

### 3.3 WBE

The wire beam electrode (WBE) was developed to monitor localized corrosion[17]. The WBE measurement has been conducted widely to determine how localized corrosion initiates and propagates as well as how such corrosion changes as corrosion inhibitors are introduced [2].

The WBE measurement produced a large amount of data. Figs. 6 and 7 only show the potential and galvanic current maps measured with the WBE in the test solutions containing no and 200 mg/L TAI at 1 h and 10 h. There are 100 data points in each galvanic current or potential distribution map. The potential gradually shifts in the positive direction with prolonged immersion time and the introduction of TAI corrosion inhibitor (Fig. 6). A positive current in Fig. 7 suggests anodic dissolution, and a negative current indicates that a cathodic reaction occurred.

The parameters, including the number of electrodes with positive current density values ( $N_a$ ), the maximum anodic current density ( $i_{\max}$ ) that indicates the worst extent of localized corrosion on the WBE surface, and the total anodic current density ( $i_{\text{tot}}$ ), which is the sum of all measured anodic current densities and indicates the overall corrosion occurring on all anodic sites, can be obtained from the potential and galvanic current maps.

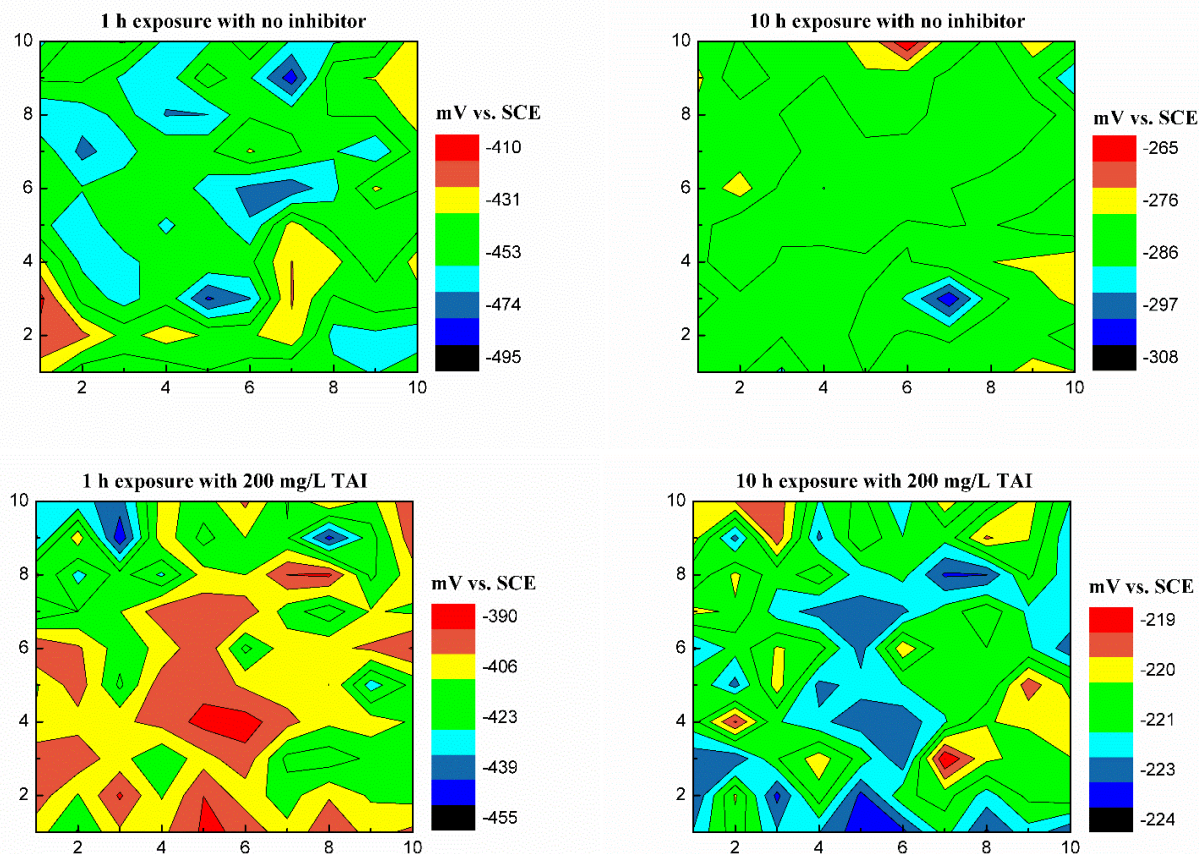


**Figure 6.** Potential maps measured on WBE exposed to the solutions containing no and 200 mg/L TAI at 1 h and 10 h.

The localized corrosion intensity index (LCII), first proposed by Tan et al.[18], can be calculated with the galvanic current data extracted from the WBE galvanic current maps using Equation 3 to quantitatively describe the intensity of localized corrosion.

$$LCII = i_{\max} / i_{\text{tot}} \tag{3}$$

For a localized corrosion system,  $i_{\max}$  is approximately equal to  $i_{\text{tot}}$ , and LCII approaches 1. For an ideally general corrosion system where the anodic current is uniformly distributed on the surfaces of all wires, the value of LCII approaches 0.01. A corrosion system with a LCII value over 0.1 can be considered highly localized.

As shown in Figs. 8 and 9, both  $i_{\max}$  and  $i_{\text{tot}}$  decreased as TAI was added, and the declines (absolute values) became more significant at higher TAI concentrations, suggesting that TAI effectively inhibited the corrosion of N80 steel. Meanwhile, the introduction of TAI, especially at a concentration of 200 mg/L, reduced the number of anodes (Fig. 10). Thus, the corrosion mainly occurred on the small amount of anodes, causing more serious pitting corrosion. Similar results were obtained by Tan et al., who also found that the number of anodes was reduced by the addition of imidazoline inhibitor in CO<sub>2</sub>-saturated 3% NaCl solution[2].

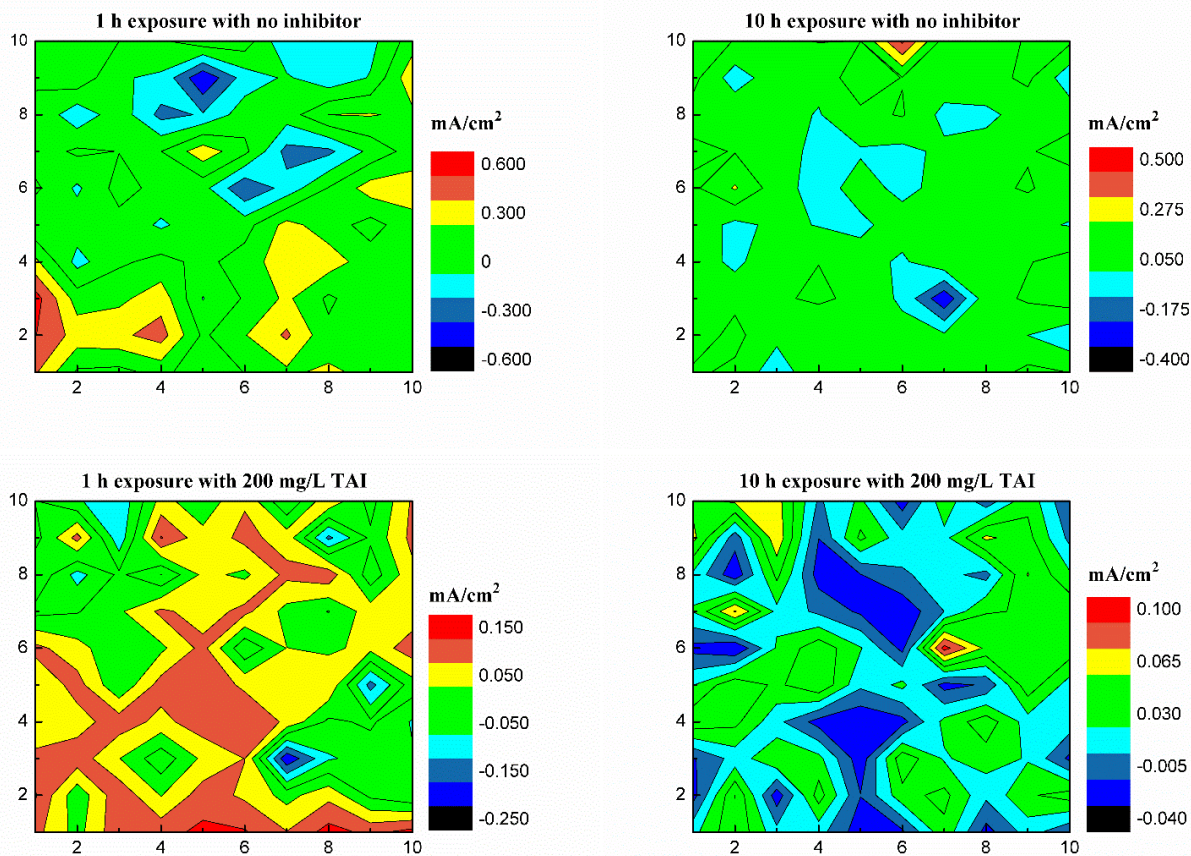


**Figure 7.** Galvanic current maps measured on WBE exposed to the solutions containing no and 200 mg/L TAI at 1 h and 10 h.

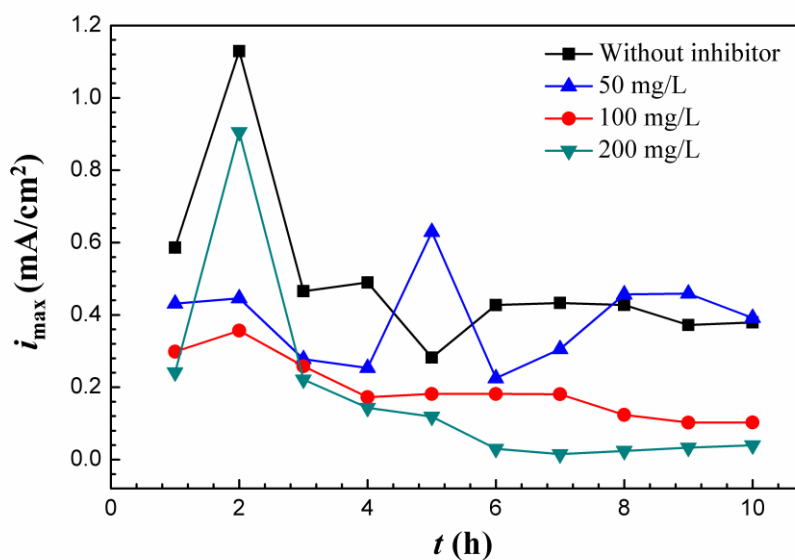


**Figure 8.**  $i_{max}$ - $t$  curves of N80 steel at different TAI concentrations

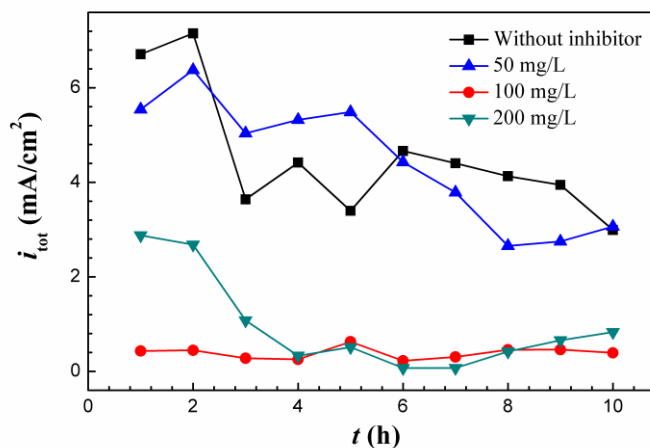


Figure 9.  $i_{tot}$ - $t$  curves at different TAI concentrations

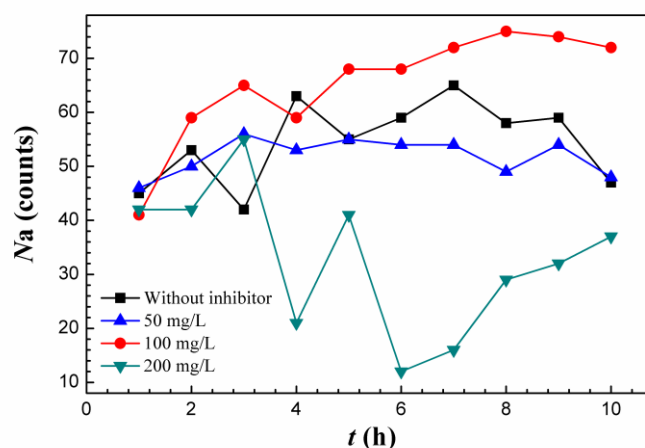


Figure 10.  $Na$ - $t$  curves at different TAI concentrations

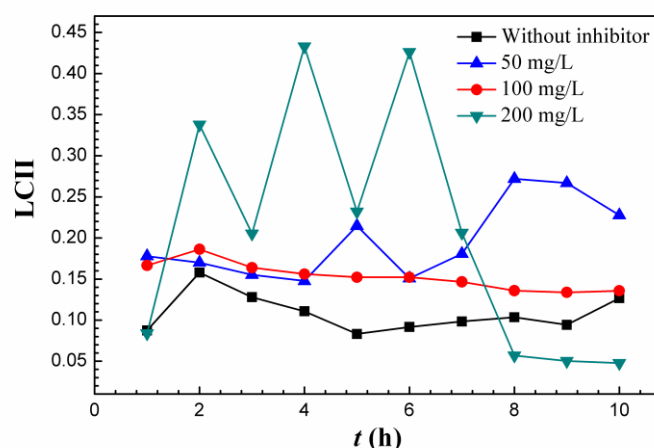


Figure 11.  $LCII$ - $t$  curves at different TAI concentrations

In addition, the addition of TAI increased the LCII of WBE (Fig. 11). For example, the LCII at TAI concentration of 200 mg/L maintained a high level in the first 5 h, suggesting that serious localized corrosion occurred. As the immersion time was further prolonged, LCII decreased, possibly due to the formation of a corrosion product layer ( $FeCO_3$ ). In all, the TAI corrosion inhibitor was able

to effectively inhibit general corrosion but increased the susceptibility to pitting corrosion, consistent with the potentiodynamic polarization and EN measurements.

#### 4. CONCLUSIONS

In summary, TAI was able to enhance the passivation while decreasing the pitting potential of N80 steel in CO<sub>2</sub>-saturated NaCl-NaNO<sub>2</sub> solution, and the pitting potential decreased with the increase of TAI concentration. TAI slowed down the general corrosion as an anodic inhibitor. The electrochemical noise resistance and localization intensity increased with the increase of TAI concentration. The number of anodes was reduced as TAI was introduced. The maximum anodic current density and total anodic current density gradually decreased, while the localized corrosion intensity index increased with the increase of TAI concentration, suggesting the increased susceptibility to pitting corrosion.

#### ACKNOWLEDGEMENT

The authors would like to thank the National Natural Science Foundation of China (No. 51471021) for the supports to this work.

#### References

1. P. Han, C. Chen, H. Yu, Y. Xu and Y. Zheng, *Corros. Sci.*, 112 (2016) 128.
2. Y. Tan, M. Mocerino and T. Paterson, *Corros. Sci.*, 53 (2011) 2041.
3. M.A. Lucio-Garcia, J.G. Gonzalez-Rodriguez, A. Martinez-Villafañe, G. Dominguez-Patiño, M.A. Neri-Flores and J.G. Chacon-Nava, *J. Appl. Electrochem.*, 40 (2010) 393.
4. B. Wang, M. Du and J. Zhang, *Adv. Mater. Res.*, 79 (2009) 981.
5. B. Wang, M. Du, J. Zhang and C.J. Gao, *Corros. Sci.*, 53 (2011) 353.
6. B. Wang, M. Du and J. Zhang, *Acta Phys.-Chim. Sin.*, 27 (2011) 120.
7. F.G. Liu, M. Du, J. Zhang and M. Qiu, *Corros. Sci.*, 51 (2009) 102.
8. J. Zhang, L. Niu, F. Zhu, C. Li and M. Du, *J. Surfact. Deterg.*, 16 (2013) 947.
9. L. Zeng, G.A. Zhang, X.P. Guo and C.W. Chai, *Corros. Sci.*, 90 (2015) 202.
10. W. S. Li and J. L. Luo, *Int. J. Electrochem. Sci.*, 2(2007) 627.
11. J. M. Zhao, Y. Zuo, *Corros. Sci.*, 44 (2002) 2119.
12. Y. Zuo, L. Yang, Y. Tan, Y. Wang and J. M. Zhao, *Corros. Sci.*, 120 (2017) 99.
13. H.H. Zhang, X.L. Pang, M. Zhou, C. Liu, L. Wei and K.W. Gao, *Appl. Surf. Sci.*, 356 (2015) 63.
14. Y.J. Tan, S. Bailey and B. Kinsella, *Corros. Sci.*, 38 (1996) 1681.
15. Y.J. Tan, S. Bailey, B. Kinsella and A. Lowe, *J. Electrochem. Soc.*, 147 (2000) 530.
16. E. García-Ochoa and J. Genesca, *Surf. Coat. Technol.*, 184 (2004) 322.
17. Y.J. Tan, *J. Electrochem. Soc.*, 156 (2009) C195.
18. Y. Tan, N.N. Aung and T. Liu, *Corros. Sci.*, 63 (2012) 379.